

Realistic Approach to Description of Signals at Output of A/D Converters

Andrzej Borys

Gdynia Maritime University, Gdynia, Poland

<https://doi.org/10.26636/jtit.2024.4.1682>

Abstract — It is common knowledge that no signals having the form of a sequence of weighted Dirac deltas, as they are currently modelled so, are present, in reality, at the output of analog-to-digital converters (ADC). No such signals are available in the otherwise large variety of physical signals. This has been illustrated in many works and shown by means of measurements. However, it is highly intriguing that the same papers (with the exception of this article) consider it necessary to model the signals at the output of ADC via sequences of Dirac deltas because only such an approach allows to describe the aliasing effect occurring in the spectra of these signals. But due to this incorrect description such an approach is obviously incomprehensible to everyone. In accepting this, however, it has been overlooked that this does not have to be the case at all. The effect of aliasing in the spectrum of a sampled signal may be explained by modeling this signal as a weighted step function. Moreover, such an approach offers also a quantitatively more accurate result for this spectrum than the one obtained using the current method. All that is illustrated in this paper that focuses on this specific theme.

Keywords — modeling ADC output signals, spectra of sampled signals

1. Introduction

Let us start by listing some facts that do not receive much attention, but are related to modeling and describing analog signals being the output signals of analog-to-digital converters (ADCs). We shall enumerate those facts and provide their brief descriptions.

It is well known that people find it difficult to understand why the time waveforms at the output of ADC have to be modelled using weighted Dirac delta series (weighted Dirac combs) despite the fact that they are considered to be step functions.

Engineers working in various industries relying on digital techniques know that analog-to-digital converters do not generate Dirac deltas. Nevertheless, the descriptions of output waveforms of ADCs are realized through non-physical objects, called Dirac deltas. Furthermore, it shall be noted that the spectrum of a sampled signal in the form of an endless repetition of the same pattern (with or without overlapping) looks rather strange. In particular, the spectra known to engineers, researchers, and students from laboratories, even if they are periodic in nature, extinguish as the frequency increases.

People often assume that when they use the formula that is currently applied, in the literature, to the spectra of sampled

signals, they deal with their Fourier transforms. However, this is not true. Such an identification of one with another often leads to misunderstandings and/or overinterpretation.

The above-mentioned ambiguities are discussed in detail in this paper. Their clarification and explanation are very important, as they allow us to correctly understand the analog signal sampling process.

Following numerous conversations and having exchanged opinions with people inventing new digital signal processing algorithms, the author of this paper has the impression that all of the above-mentioned ambiguities are considered irrelevant by his interlocutors who do not attach much attention to them. Such an approach of those researchers may be partly understandable, but only in cases in which they work with signals they understand as functions of a discrete variable, leaving aside the existence of a physical time. Using mathematical terminology, one may say that they then operate in the spaces of discrete functions only.

The trouble is that they continuously switch from their solutions in the form of functions of a discrete variable to functions of a continuous variable, denoting a continuous time t belonging to the set of real numbers, and vice versa. In other words, the researchers move directly with their solutions from the spaces of discrete functions to the spaces of functions of a continuous variable, and vice versa. But this can generate errors and indeed it does. However, these errors are marginalized or ignored.

It seems that this approach should be given a closer look as far as signal processing is concerned, primarily due to the very simple reason that while focusing on this area, we always measure and/or use signals that are functions of a continuous real time variable t , and are not function of an abstract discrete variable. This is also the case when we talk about the so-called discrete time and/or consider the measurement process to be a specific type of sampling of an analog signal.

The so-called discrete time, a concept used in digital signal processing, must then be understood as a set of ordered discrete time instants “immersed” in a continuous real-time axis. It is “embedded in this axis, built into this time context” and should be interpreted as more than merely a set of ordered discrete values [1].

Moreover, as shown in [2] and [3], if we perceive the process of measuring a physical signal to be similar to the sampling of an analog signal and model it as such, then this “sampled” signal must be understood as a function of a continuous real

time variable t , e.g. it must be a step function of variable t or must have a similar form, but cannot be a sequence of the weighted time-shifted Dirac deltas.

Therefore, all the ambiguities listed at the beginning of this section are directly related to proper perception, description, and modeling of the signals that are used in various electronic signal processing devices. Furthermore, because of the relationships just mentioned above, explaining those ambiguities is of vital importance for all people dealing with signal processing. With that taken into consideration, this is exactly one of the main objectives of this paper.

It is also worth noting that since digital-to-analog (D/A) conversions are the reverse of A/D operations, the considerations presented in this paper are also directly applicable to modeling the former [4].

The remainder of this paper is organized as follows. In Sections 2–4, pitfalls related to modeling operations performed with the use of weighted Dirac and Kronecker sequences, as well as taking into account improperly nonidealities of the sampling process, are presented. Sections 5 and 6 are devoted to modeling ADC output waveforms via step functions, and to presenting measurement results confirming the reliability of this model. In Section 7, calculations of the spectra of the aforementioned signals are discussed. The paper ends with some conclusions and remarks in Section 8.

2. Modeling Relying on Dirac Deltas

The process of modeling time waveforms at the output of A/D converters with the use of Dirac deltas is widely assumed to be the only correct approach. It is worth noting that this method is taught to students all over the world, including the USA [5]. In this context, let us mention a couple of very well-known textbooks [6]–[10] that promote this approach.

The method of modeling a sampled signal in the space of a continuous time t with the use of replicated weighted Dirac deltas is illustrated in Fig. 1. This signal is called $x_T(t)$.

Further, in the context of the visualization shown in Fig. 1, it is also worth noting that the upper curve in this figure is nothing else but the so-called Dirac comb shown in Fig. 2 and denoted as $\delta_T(t)$, multiplied by the values of samples of signal $x(t)$ – see the lower curve in Fig. 1.

The Dirac delta is defined in many ways in the literature. One of those definitions uses the notion of a functional. In such a context, one may write:

$$\langle \delta, z \rangle = \int_{-\infty}^{\infty} \delta(\tau) z(\tau) d\tau = z(0), \quad (1)$$

where δ stands for the Dirac delta (Dirac pulse) and z is a test function, respectively.

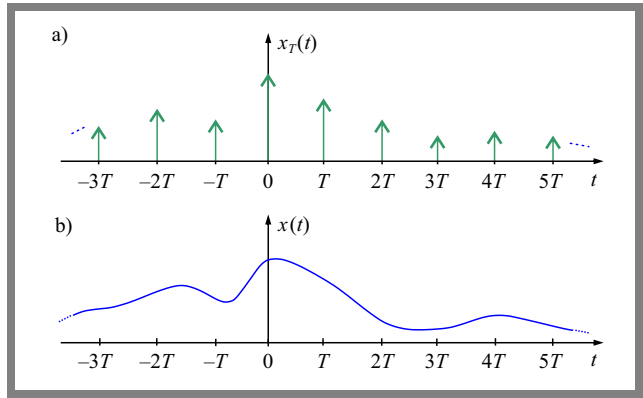


Fig. 1. Example sampled signal a) in the form of a series of weighted Dirac deltas occurring uniformly along the continuous time axis, at intervals T from each other, and its un-sampled version b), where t stands for a continuous time variable [11].

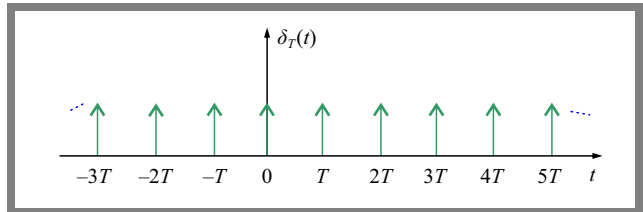


Fig. 2. Visualization of the Dirac comb being a series (sum) of Dirac deltas replicated uniformly along the continuous time axis, at T intervals [11].

Further, note that a shifted Dirac delta multiplied by a constant $x(kT)$ is given by:

$$\begin{aligned} \langle x(kT) \delta(\tau - kT), z \rangle &= \int_{-\infty}^{\infty} x(kT) \delta(\tau - kT) z(\tau) d\tau, \quad (2) \\ &= x(kT) z(kT) = x(kT) \neq \infty \end{aligned}$$

with $z(kT) = 1$. In Eq. (2), T is the sampling period of an analog signal $x(t)$ of a continuous time t , k is an integer, i.e. $k \in \{\dots, -2, -1, 0, 1, 2, \dots\}$.

With the context presented above taken into consideration, one needs to note that this non-physical and abstract object referred to as the Dirac delta (a.k.a. Dirac pulse or Dirac distribution), not being a function, is defined – for teaching-related purposes – as follows:

$$\delta(t - kT) = \begin{cases} \infty & \text{for } t = kT \\ 0 & \text{otherwise} \end{cases}, \quad (3)$$

as it is a common opinion that engineers are not able to correctly understand a sophisticated theory of distributions originally devised by L. Schwartz and developed further by other researchers.

At this point, let us refer to one example, taken from [12]. According to the research findings presented therein, an integral of the Dirac delta exists and is given by:

$$\int_{-\infty}^{\infty} \delta(t - kT) dt = 1. \quad (4)$$

In fact, the integrals from Eqs. (1), (2) and (4), with δ understood in the manner given in Eq. (3), do not exist in the Riemann sense or are equal to zero in the Lebesgue sense. Thus, they can only play a role of symbols of certain operations there.

The approach mentioned above, relied upon when teaching engineers, is called “primitive” – see, for instance, the textbook by Hoskins [13]. It is also adopted at the Massachusetts Institute of Technology (MIT) [5].

The fact that they have to deal with (observe) finite values equal to $x(kT)$ (with some tolerance) at the sampling instants kT is undoubtedly shocking to engineers, but according to Fig. 1a, they are to believe that these values of the signal samples amount to $x(kT) \delta(\tau - kT)$, respectively, with the same values being, in another interpretation, infinite or undefined simultaneously. This shows that we are dealing with a contradiction here. Therefore, the argumentation presented above is absolutely not understandable to engineers.

The fact that the values of the waveform shown in Fig. 1a for time instants differing from kT are identically equal to zero is another drawback of the model with the Dirac deltas.

Obviously, the above is not true, as the values of the signal samples do not disappear at the outputs of ADCs outside the sampling instances. One may assume that they remain the same (constant) between the successive signal sampling instants.

3. Kronecker Functions in Modeling

The first drawback of the model with the Dirac deltas may be easily removed by simply describing the signal samples at the time sampling instants kT , as we observe (measure) them. Then, we get a model illustrated by the function shown $x_{K,T}(t)$ in Fig. 3. And we notice that we have a weighted comb of the so-called Kronecker functions (Kronecker deltas), weighted by the values of signal samples.

The definition of the Kronecker function is given by:

$$\delta_{k, \frac{t}{T}}(t) = \begin{cases} 1 & \text{if } k = \frac{t}{T} \\ 0 & \text{otherwise} \end{cases}, \quad (5)$$

where k is an integer, while t represents a real number.

The problem with the type of modeling presented in Fig. 3 is the following. The signal shown in this figure does not have a spectrum (understood as its Fourier transform) when Riemann integrals are used in its definition, or is equal to zero when Lebesgue integrals are used.

The remedy in this case may be to adopt a common-sense definition of the spectrum by choosing some relation to the Fourier transform of the related signal, provided that the latter exists, of course.

Additionally, when looking at Fig. 1a and Fig. 3a, it is also worth noting that they are similar. This does not mean, however, that they are the same. Both represent “modulated” combs. In the first case, it is a Dirac comb, while in the other, a Kronecker comb; the latter is visualized in Fig. 4 and

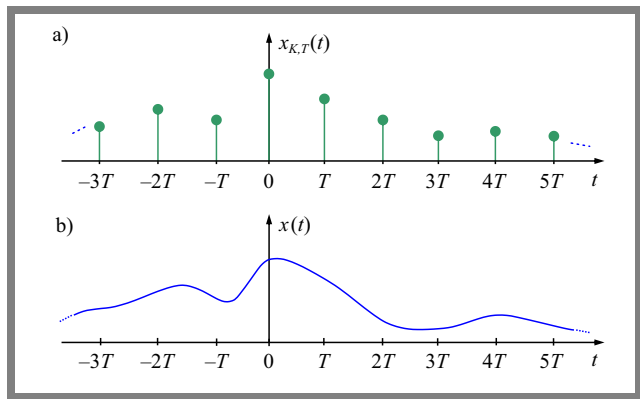


Fig. 3. Example sampled signal a) in form of a series of signal samples occurring uniformly along the continuous time axis, at intervals T , and its un-sampled version b) [14].

denoted as $\delta_{K,T}(t)$. Note that the difference between both scenarios consists in the fact that the former has infinite values at the sampling instants, whereas the latter has finite ones. These finite values equal ones.

Now, returning to the previous statement and proposition (given immediately before Fig. 3), one may say that the relation mentioned there can be (theoretically) of any variety. So, in this case, we are dealing with an ambiguity of the proposed method. Therefore, it cannot be accepted.

By the way, one should note that this is exactly the method used to define the spectrum of a signal at the output of an ADC by using a closely related signal that exploits the Dirac deltas (Fig. 1) in its description, for which there exists a Fourier transform (as mathematicians prove in a distributional sense). It is the signal that is “closely” related with the one shown in Fig. 3a.

In other words, in this spectrum calculation procedure, we take the signal shown in Fig. 1a instead of the one presented in Fig. 3a. For the reason described above, i.e. due to the lack of success in applying the above approach, it was necessary to continue the search for a proper description of the sampled signal, i.e. of the signal occurring at the ADC output. Such a search was undertaken by the author. The results of these efforts are described in the following sections.

4. Proper Description Based on Analyzing the Non-ideal Sampling Process

The most relevant proposals concerning the modeling of non-ideal behavior of the process of sampling an analog

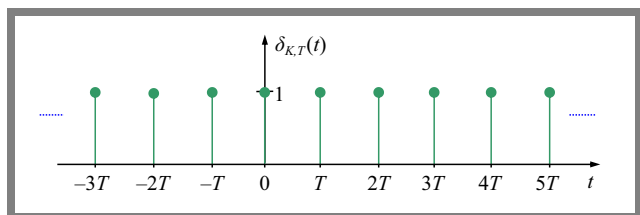


Fig. 4. Visualization of the Kronecker comb – the series (sum) of Kronecker functions, also known as Kronecker deltas, forms the Kronecker comb [14].

signal using ADC are described (among others) in [15]. They consider two non-idealities of the sampling process, namely: the fact that the signal sampling time τ in ADC is finite (1) and the samples obtained are blurred (smeared) (2).

The author of this paper has taken a closer look at the non-idealities mentioned above to check their potential applicability in obtaining such a description of the sampled signal which makes it possible to correctly calculate the spectrum of the actual signal occurring at the ADC output. Detailed results of this search were presented in [14] and [16]. Here, only the resulting conclusions are mentioned.

The inconveniences of modeling a sampled signal using the above-mentioned non-idealities are most apparent when the ideal case is considered. Thus, in the first case, the spectrum of this signal is directly proportional to the sampling time τ . So, when τ moves towards zero, the spectrum also moves towards zero, and for the value of $\tau = 0$, it is equal to zero. Therefore, only one conclusion may be drawn from this fact: this kind of modeling diverges from reality and should be considered useless.

In the case of the other non-ideality mentioned above, its idealization means that the blurring effect of the signal samples is getting smaller and smaller, or that the effective blurring time of the signal samples decreases to zero. Consequently, the blurred signal samples become more and more similar to weighted Dirac impulses. That is, here, in the limiting case, it turns out that we are modeling a signal sampled with a weighted Dirac comb – an approach that was criticized previously.

It is possible to combine both of the non-idealities listed above, i.e. to approach cases 1 and 2 together, assuming that they occur at the same time. This was done in [16] and a rather unexpected result was obtained, according to which this modeling method leads to a description of the sampled signal in the form of a weighted Kronecker comb. This outcome is unsatisfactory as well, due to the reasons given in Section 4.

5. Description of ADC Output Waveforms via Step Functions

A brief analysis of the proposals concerning the modeling the sampled signal, applied in the calculation of the spectrum of the ADC output signal, as presented in Section 4, leads to the conclusion that such a method also does not yield positive results. A closer look reveals that this is due to the fact that in these models, during the periods between taking the sample values, all other signal values are zero (in the ideal variant of a given model), mostly zero or close to zero (in the non-ideal variant of a given model).

It seems to us that in order to provide a correct answer to the problem discussed in this paper, the best way is to refer, in the first instance, to the reality of the sampling process as it is implemented in an A/D converter. This is illustrated schematically in Figs. 5 and 6 which allow us to understand the operation of the converter and the time waveforms, as

functions of a continuous time t , that it generates at its output. One can assume that these time waveforms have the form of a slightly disturbed step function presented in Fig. 7. In Fig. 7, $[x_{s,H}(-3T)]_Q$ and $[x_{s,H}(T)]_Q$, where the lower index Q means the amplitude quantization operation, illustrate the quantized values of the sampled signal $x_s(t)$. These values are assigned to the following instants: $-3T$ and T , respectively. Moreover, parameter τ can be identified with the sum of the track part and the beginning of the hold part of an actual output signal at the output of ADC, at the time at which the sampling of a signal takes place [4], [17].

The shape of actual waveforms at the outputs of A/D converters is richer than the step function shown in Fig. 7 and depends upon the architecture and technology a given A/D converter relies upon. This shape is characterized by such parameters as: settling time, acquisition time, aperture, aperture jitter, hold mode settling time, hold mode feedthrough, droop [4]. The values of those parameters may be relevant in signal processing specific applications [19]–[21].

In view of the above, one may say that the problem can be formulated as: how to best model physical reality. And according to this, do the following:

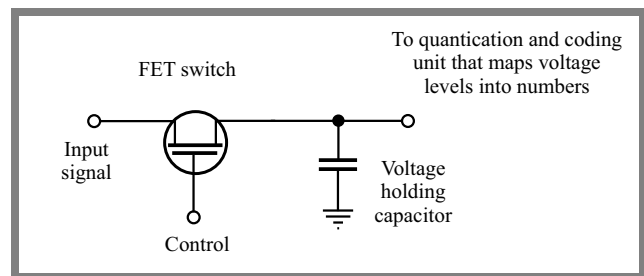


Fig. 5. Illustration of the basic idea behind analog-to-digital conversion with the use of a FET transistor switch connected to a capacitor holding the value of an analog input signal taken at the time of switching [18].

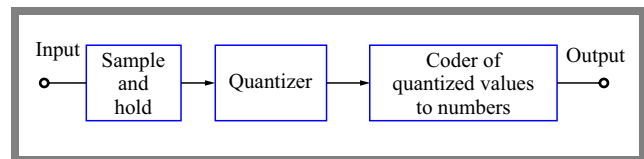


Fig. 6. Block diagram of an A/D converter consisting of three blocks: a sample and hold unit, an amplitude quantization stage, and a mapper (coder) of quantized values to numbers [4].

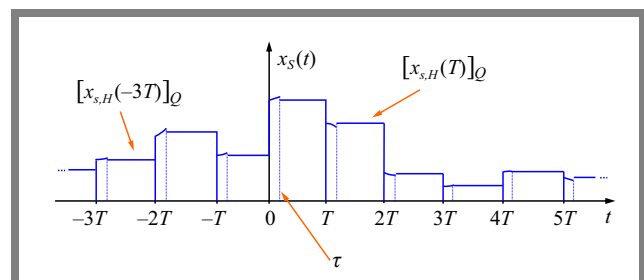


Fig. 7. Time waveform of an example sampled signal $x_s(t)$, related with an un-sampled one $x(t)$ (not shown).

- perform the signal averaging operation on a part of or the entire signal between the successive signal samples, to get a clearer picture,
- treat the difference between the sample value and the averaged value as a constant error over a given sampling period,
- treat, for each time instant, the difference between the value of the output signal of an A/D converter and the sum of the constant error mentioned above and the averaged value as a value of an error (we may refer to it as overall noise) for that time instant in the period between the successive sampling instants,
- realize that the value of the signal sample remains, throughout the entire period, between the successive sampling times, with the overall noise changing around this value.

Note that the application of the above procedure leads to the following analytical description of the time waveform at the ADC output:

$$x_g(t) = x_g(kT) \text{ for } kT \leq t < (k+1)T \text{ and } k = \left\lfloor \frac{t}{T} \right\rfloor, \quad (6)$$

where the lower index g in $x_g(t)$ stands for “general” as well as for “generic”.

In Eq. (6), $x_g(t)$ means $x(kT) + \text{bias}(kT)$ for the subsequent periods. This formula is general in nature because it correctly describes, in a completely general manner, the time waveforms at the output of A/D converters. It is also generic, because it is “ready” – see the $\text{bias}(kT)$ component mentioned above – to take into account different forms of the error function, which will obviously depend upon the architecture and technology used in the implementation of a given ADC [4], [19]–[21]. Interestingly, it may also depend upon the sampling frequency [19]. Furthermore, when assuming that the bias is identically equal to zero, then, obviously, $x_g(kT) \equiv x(kT)$. Note also that this parameter, referred to as bias, is constant in a given time period between the successive sampling instants, but not necessarily in all of these periods.

6. Measurement-based Validation of the Model

The fact that the waveforms at outputs of A/D converters may be considered weighted step functions, i.e. being good approximations of their real-world counterparts, has been noted in various research papers. Here, we place an emphasis on several of them, namely to [18] and [22]–[26].

For the purpose of this paper, in order to demonstrate the validity of the model presented in Section 5 and description of the waveforms at the output of A/D converters, a series of measurements was performed.

The measurements were carried out using the TMS320C5515 eZdsp 16-bit DSP runtime platform, i.e. a development tool for the TMS320C5515 DSP equipped with the AIC3204 codec, containing two 16-bit ADCs. In the course of the measurement campaign, one of the available ADCs was used.

The planned experiments performed with the use of the TMS320C5515 eZdsp development tool were subject to several limitations. Firstly, the number of quantization steps could not be lowered to better illustrate the step-like nature of the waveforms from initial resolution, i.e. 65536 quantization steps. Secondly, the sampling frequency could not be arbitrarily set. Thirdly, it was not possible to connect an oscilloscope to the ADC output in the AIC3204 codec.

With such shortcomings affecting the sampling frequency, the highest value offered in TMS320C5515 eZdsp, i.e. 192 kHz was selected to ensure a sufficiently high resolution on the time axis of the waveform diagrams. Further, signals with very small amplitudes were sampled to ensure transparency and visibility of details on the ordinate axis, i.e. with the changing amplitude of the waveform. Therefore, the amplitude of a signal “passed” through a low number of quantization steps only, at the expense of exposing this signal to a high level of noise, close to the values of its changing amplitude. Finally, as for the oscilloscope, we used a virtual programmable block that can be designed using the TMS320C5515 eZdsp software.

In Figs. 8–9, two series of example signal waveforms at the output of the A/D converter are presented, as recorded for two sinusoidal signals sample: the first with the frequency of 2 kHz and the other with the frequency of 5 kHz.

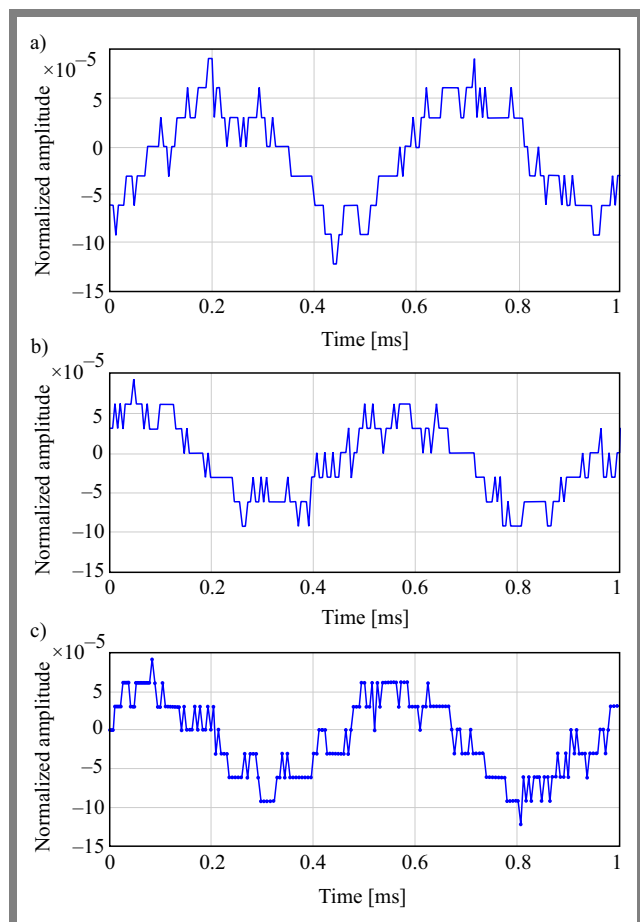


Fig. 8. Waveform recorded for a 2 kHz sinusoidal signal: a) first, b) second, and c) third one, where signal samples are marked by dots.

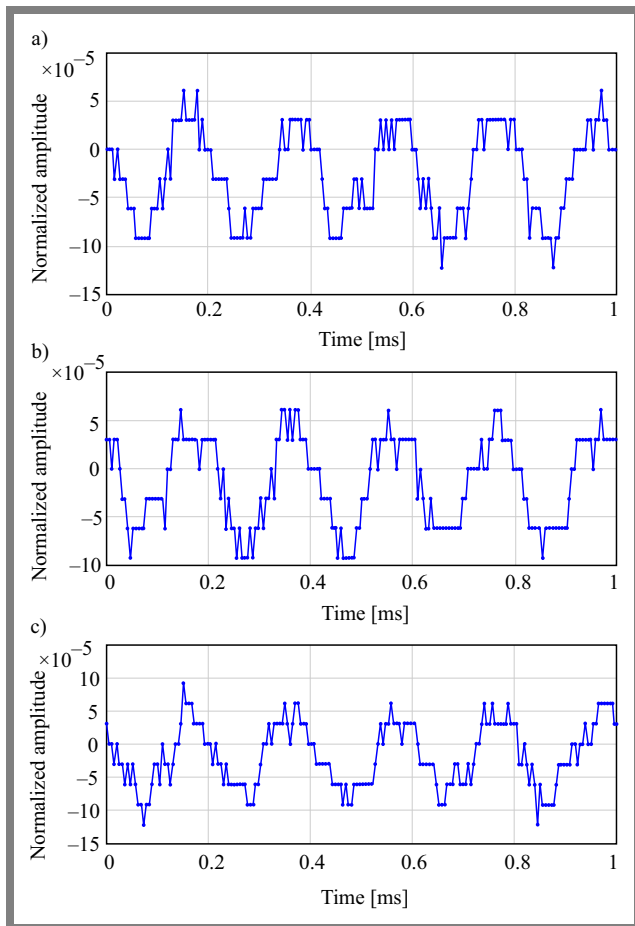


Fig. 9. Recorded waveform for a 5 kHz sinusoidal signal with sample values denoted by dots: a) first, b) second, and c) third instance.

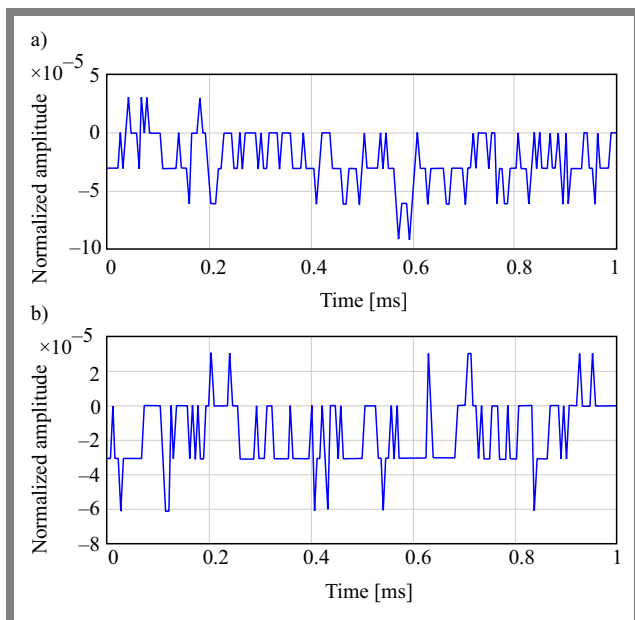


Fig. 10. Example of a noise waveform recorded using the oscilloscope: a) first and b) second instance.

Figures 8–9 show normalized amplitude values presented as quantized levels. Quantization mapping was performed using the Q1.15 format. So, in this case, the range that can

be covered extends from -1 to 0.99997 , with a resolution of $2^{-15}=0.0000305$.

Figures 8–9 show also a non-ideal operation of the virtual oscilloscope used. Its time resolution equals $(192000)^{-1} \text{ s} \simeq 5.2 \text{ ns}$. Therefore, the signal amplitude values for adjacent (i.e. closest to each other) time instants following from this resolution are connected by a straight line. The sloping segments of straight lines, clearly visible at numerous locations, make it difficult to interpret the presented waveforms.

The waveforms presented in Figs. 8–9 show a significant influence of noise that is added to the useful signal and changes the output code of the ADC converter. Figure 10 allows to assess the noise level presenting on ADC output for two examples of a zero-valued signal at the input. One may notice that the level is high and its value is equal to four quantization steps. This is a large value compared to the value of the same measure for the sampled useful signal, which was eight quantization steps (see Figs. 8–9). Such a noise cannot be eliminated by subtraction from the useful signal, because the noise is random and the useful signal is deterministic. The second remark concerns the way in which Figs. 8–9 as well as Fig. 10 illustrate the transition between the quantization levels, using an inclined straight-line segment. It may not be very transparent, but it is not so difficult to imagine that at these locations significant up or down shifts occur for the neighboring time instants.

One may conclude that due to the curves observed in these figures (leaving aside the influence of noise), we are dealing with sinusoidal waveforms in which step functions (with their change values being lower than the amplitudes of the sinusoids themselves) are inscribed. This means that the model description of the sampled signal presented in the previous section and illustrated in Fig. 7 is correct and that its validity has been demonstrated by measurements.

7. Calculation of the Sampled Signal Spectrum

Calculation of the Fourier transform of function $x_g(t)$, i.e. its spectrum which is a step function, does not present any problems, as it is a function for which the Fourier transform (understood in a classical form) exists. In the following calculations, we present the main steps of the process.

Let us start with a basic formula:

$$\begin{aligned}
 X_g(f) &= \mathcal{F}(x_g(t)) = \int_{-\infty}^{\infty} x_g(t) e^{-j2\pi ft} dt = \\
 &= \dots + \int_{-T}^0 x_g(-T) e^{-j2\pi ft} dt + \int_0^T x_g(0) \\
 &\times e^{-j2\pi ft} dt + \int_T^{2T} x_g(T) e^{-j2\pi ft} dt + \dots
 \end{aligned} \tag{7}$$

Then, calculation of the integrals in Eq. (7) leads to:

$$\begin{aligned}
 X_g(f) = & \dots + \frac{x_g(-T)}{-j2\pi f} e^{-j2\pi f t} \Big|_{-T}^0 \\
 & + \frac{x_g(0T)}{-j2\pi f} e^{-j2\pi f t} \Big|_0^T + \frac{x_g(T)}{-j2\pi f} \\
 & \times e^{-j2\pi f t} \Big|_T^{2T} + \dots = \frac{j}{2\pi f} \left\{ \dots - x_g(-T) e^{j2\pi f T} \right. \\
 & + x_g(-T) e^{-j2\pi f(0T)} - x_g(0T) e^{-j2\pi f(0T)} \\
 & + x_g(0T) e^{-j2\pi f T} - x_g(T) e^{-j2\pi f T} + x_g(T) \\
 & \times e^{-j2\pi f(2T)} + \dots \left. \right\} = \frac{j}{2\pi f} \left\{ \dots + [x_g(-2T) - x_g(-T)] \right. \\
 & \times e^{j2\pi f T} + [x_g(-T) - x_g(0T)] e^{j2\pi f(0T)} \\
 & + [x_g(0T) - x_g(T)] e^{-j2\pi f T} + [x_g(T) - x_g(2T)] \\
 & \times e^{-j2\pi f(2T)} + \dots \left. \right\}. \tag{8}
 \end{aligned}$$

With the use of the definition of DTFT, Eq. (8) can be rewritten as:

$$X_g(f) = \frac{1}{j2\pi f} \left\{ \text{DTFT}(x_g(kT)) - \text{DTFT}(x_g((k-1)T)) \right\} \tag{9}$$

Moreover, we can write:

$$\begin{aligned}
 \text{DTFT}(x_g((k-1)T)) &= \sum_{k=-\infty}^{\infty} x_g((k-1)T) \\
 &\times e^{-j2\pi f k T} = \sum_{k'=-\infty}^{\infty} x_g(k'T) \\
 &\times e^{-j2\pi f(k'+1)T} = e^{-j2\pi f T} \\
 &\times \sum_{k'=-\infty}^{\infty} x_g(k'T) e^{-j2\pi f k' T} \\
 &= \text{DTFT}(x_g(kT)) e^{-j2\pi f T}. \tag{10}
 \end{aligned}$$

Further, introducing Eq. (10) into Eq. (9) we get:

$$\begin{aligned}
 X_g(f) &= \frac{\text{DTFT}(x_g(kT))}{j2\pi f} (1 - e^{-j2\pi f T}) \\
 &= T \cdot \text{DTFT}(x_g(kT)) \frac{e^{j\pi f T} - e^{-j\pi f T}}{j2\pi f T e^{j\pi f T}} \\
 &= T \cdot \text{DTFT}(x_g(kT)) e^{-j\pi f T} \frac{\sin(\pi f T)}{\pi f T} \\
 &= T \cdot \text{DTFT}(x_g(kT)) \text{sinc}(\pi f T) e^{-j\pi f T}. \tag{11}
 \end{aligned}$$

The final form may be determined as:

$$X_g(f) = T \cdot \text{DTFT}(x_g(kT)) \text{sinc}(\pi f T) e^{-j\pi f T}. \tag{12}$$

Let us consider a special case $\frac{f}{f_s} \ll 1 \rightarrow f \ll f_s$, where $f_s = \frac{1}{T}$. We can then simplify the expression given by Eq. (12) to:

$$X_g(f) \cong T \cdot \text{DTFT}(x_g(kT)). \tag{13}$$

For $f \gg f_s$, we can write:

$$X_g(f) \cong 0. \tag{14}$$

For the frequencies lying between the ranges mentioned above, the full formula given by Eq. (12) must be used.

Note that the above means a low-pass filtering character of the influence of the function $\text{sinc}(\pi f T)$ in changing DTFT to arrive at $X_g(f)$. Finally, we shall draw the reader's attention to another interesting relationship. It is well known that a relationship exists between the DTFT of a discrete time signal and the spectrum of its un-sampled version, say $X(f)$. It has the following form:

$$\text{DTFT} = \frac{1}{T} \sum_{k=-\infty}^{\infty} X(f - kf_s). \tag{15}$$

Using this expression in Eq. (12), we get:

$$X_g(f) = \text{sinc}(\pi f T) e^{-j\pi f T} \times \sum_{k=-\infty}^{\infty} X(f - kf_s). \tag{16}$$

In view of the results achieved in this paper, formula (16), rather than the one given in Eq. (15), should be used in any analyses of the aliasing effects in the frequency domain.

8. Conclusions and Remarks

It has been shown in this paper that the description of the signals at the outputs of A/D converters, using the weighted Dirac combs, suffers from two severe drawbacks. The most satisfactory description relies on modeling A/D behavior that fully complies with the realities of the physical sampling process. It uses step functions instead of Dirac deltas.

Finally, a modified formula for calculation of the spectrum of a signal at the output of an A/D converter has been derived, in follow up to [27], better describing the spectrum of the A/D converter output signal through the spectrum of the un-sampled waveform and its aliases.

Acknowledgment

The author of this paper would like to thank his colleague, Andrzej Łuksza, Ph.D. for performing the measurements presented in this paper and for agreeing to their publication.


References

- [1] A. Borys, "Some Topological Aspects of Sampling Theorem and Reconstruction Formula", *International Journal of Electronics and Telecommunications*, vol. 66, no. 2, pp. 301–307, 2020 (<https://doi.org/10.24425/ijet.2020.131878>).
- [2] A. Borys, "Measuring Process via Sampling of Signals, and Functions with Attributes", *International Journal of Electronics and Telecommunications*, vol. 66, no. 2, pp. 309–314, 2020 (<https://doi.org/10.24425/ijet.2020.131879>).

- [3] A. Borys, "Further Discussion on Modeling of Measuring Process via Sampling of Signals", *International Journal of Electronics and Telecommunications*, vol. 66, no. 3, pp. 507–513, 2020 (<https://doi.org/10.24425/ijet.2020.134006>).
- [4] R. van de Plassche, *Integrated Analog-To-Digital and Digital-To-Analog Converters*, Berlin: Springer Verlag, 501 p., 1994 (<https://doi.org/10.1007/978-1-4615-2748-0>).
- [5] MIT, OpenCourseWare, "Signal Processing – Continuous and Discrete", [Online]. Available: <https://ocw.mit.edu/courses/2-161-signal-processing-continuous-and-discrete-fall-2008/pages/readings/>.
- [6] J.H. McClellan, R. Schafer, and M. Yoder, *DSP First*, London: Pearson, 2015 (ISBN: 9780136019251).
- [7] V.K. Ingle and J.G. Proakis, *Digital Signal Processing Using Matlab*, 3rd ed., Stamford: Cengage Learning, 672 p., 2011 (ISBN: 9781111427375).
- [8] R.J. Marks II, *Introduction to Shannon Sampling and Interpolation Theory*, New York: Springer-Verlag, 324 p., 1991 (<https://doi.org/10.1007/978-1-4613-9708-3>).
- [9] R.N. Bracewell, *The Fourier Transform and Its Applications*, 3rd ed., New York: McGraw-Hill, 640 p., 2000 (ISBN: 9780073039381).
- [10] R. Brigola, *Fourier-Analysis und Distributionen: Eine Einführung mit Anwendungen*, Hamburg: Tredition, 448 p., 2013 (ISBN: 9783847287421) (in German).
- [11] A. Borys, "Spectrum Aliasing does not Occur in Case of Ideal Signal Sampling", *International Journal of Electronics and Telecommunications*, vol. 67, no. 1, pp. 71–77, 2021 (<https://doi.org/10.24425/ijet.2021.135946>).
- [12] S.C. Gupta, "Delta Function", *IEEE Transactions on Education*, vol. 7, no. 1, pp. 16–22, 1964 (<https://doi.org/10.1109/TE.1964.4321835>).
- [13] R.F. Hoskins, *Delta Functions: An Introduction to Generalized Functions*, Oxford: Woodhead Publishing, 280 p., 2010 (ISBN: 9781904275398).
- [14] A. Borys, "Spectrum Aliasing does Occur only in Case of Non-ideal Signal Sampling", *International Journal of Electronics and Telecommunications*, vol. 67, no. 1, pp. 79–85, 2021 (<https://doi.org/10.24425/ijet.2021.135947>).
- [15] A. Dąbrowski, "Fundamentals of Systems, Signals and Information Theory: Sampling of Signals", Department of Control and Systems Engineering, Technical University of Poznań, Poland, 2008.
- [16] A. Borys, "An Unexpected Result on Modelling the Behavior of A/D Converters and the Signals They Produce", *International Journal of Electronics and Telecommunications*, vol. 69, no. 1, pp. 193–198, 2023 (<https://doi.org/10.24425/ijet.2023.144350>).
- [17] A. Borys, "Sampled Signal Description That is Used in Calculation of Spectrum of This Signal Needs Revision", *International Journal of Electronics and Telecommunications*, vol. 69, no. 2, pp. 319–324, 2023 (<https://doi.org/10.24425/ijet.2023.144367>).
- [18] P. Prandoni and M. Vetterli, *Signal Processing for Communications*, Lausanne: EPFL Press, 371 p., 2008 (ISBN: 9781420070460).
- [19] N. Ma *et al.*, "Influence of Sampling Frequency on Magneto-optical Imaging under Alternating Magnetic Field Excitation", *IEEE Sensors Journal*, vol. 19, no. 23, pp. 11591–11600, 2019 (<https://doi.org/10.1109/JSEN.2019.2937629>).
- [20] K. Sozański, *Digital Signal Processing in Power Electronics Control Circuits*, London: Springer-Verlag, 285 p., 2013 (ISBN: 9781447152668).
- [21] T.S. Low and C. Bi, "Design of A/D Converters with Hierarchic Networks", *IEEE Transactions on Industrial Electronics*, vol. 43, no. 1, pp. 184–191, 1996 (<https://doi.org/10.1109/41.481424>).
- [22] MathWorks, "Switched Capacitor Analog to Digital Converter", [Online]. Available: <https://www.mathworks.com/help/sps/ug/switched-capacitor-analog-to-digital-converter.html>.
- [23] A. Mertins, *Signaltheorie: Grundlagen der Signalbeschreibung, Filterbänke, Wavelets, Zeit-Frequenz-Analyse, Parameter- und Signalschätzung*. Berlin: Springer Verlag, 461 p., 2020 (<https://doi.org/10.1007/978-3-658-29648-3>) (in German).
- [24] U. Zölzer, *Digital Audio Signal Processing*, Chichester: Wiley & Sons, 340 p., 2008 (ISBN: 9780470997857).
- [25] C. Marven and G. Ewers, *A Simple Approach to Digital Signal Processing*, Hoboken: Wiley-Interscience, 236 p., 1996 (ISBN: 9780471152439).
- [26] SlideServe, "Analog/Digital Conversion", [Online]. Available: <https://www.slideserve.com/papaj/analog-digital-conversion-powerpoint-ppt-presentation>.
- [27] A. Borys, "A New Result on Description of the Spectrum of a Sampled Signal", *International Journal on Marine Navigation and Safety of Sea Transportation*, vol. 18, no. 2, 2024 (<https://doi.org/10.12716/1001.18.02.17>).

Andrzej Borys, Ph.D.

Faculty of Electrical Engineering

 <https://orcid.org/0000-0003-1316-4031>

 E-mail: a.borys@we.umg.edu.pl

Gdynia Maritime University, Gdynia, Poland

<https://umg.edu.pl/en/>